Steady-Shear Rheology of Block Copolymer Melts: Zero-Shear Viscosity and Shear Disordering in Body-Centered-Cubic Systems

John M. Sebastian,[†,§] Chiajen Lai,[⊥,†] William W. Graessley,[†] and Richard A. Register[*,†,‡]

Department of Chemical Engineering and Princeton Materials Institute, Princeton University, Princeton, New Jersey 08544

Gary R. Marchand[#]

The Dow Chemical Company, P.O. Box 400, Plaquemine, Louisiana 70765

Received August 24, 2001; Revised Manuscript Received November 28, 2001

ABSTRACT: The steady-shear rheology of polystyrene−polyisoprene (S/I) block copolymer melts having a body-centered-cubic (bcc) morphology has been characterized as a function of applied shear stress. At temperatures below the order−disorder transition (ODT) and at low stresses ($\tau < 100$ Pa), both diblocks and triblocks manifest finite but extremely large ($\eta_0 = 10^7-10^8$ Pa·s) zero-shear viscosities. Small-angle X-ray scattering (SAXS) measurements indicate that at these low stresses the bcc lattice remains intact. This Newtonian region ends abruptly when a critical shear stress is reached ($\tau_c \approx 200$ Pa), the steady shear viscosity decreasing by almost 4 orders of magnitude with only a factor of 3 further increase in stress. The viscosity then enters a weakly shear-thinning regime very similar to the behavior of the same block copolymer above its ODT temperature. As shown by SAXS, there is no lattice order in this high-stress regime, indicating that "shear-disordering" has occurred. If the disordered polymer is held fixed or subjected to a low stress ($\tau < 100$ Pa), it gradually regains its original equilibrium state, following the same kinetics as after a thermal quench from above to below the ODT temperature.

I. Introduction

Block copolymer melts in a microphase-separated state exhibit complex flow behavior. Numerous experimental studies and theoretical models have attempted to elucidate the intimate coupling between rheology and morphology. However, as described in several recent literature reviews,[1−5] this interrelationship is sensitive to a wide range of variables, and a fundamental and comprehensive understanding has yet to be realized. This is certainly true for highly asymmetric block copolymers—the materials of interest in this study—whose equilibrium microphase-separated structure consists of spheres of the minority component packed onto a body-centered-cubic lattice.

The fundamental question we address here is the behavior of sphere-forming block copolymers at low deformation rates. In the quiescently ordered state, and at the lowest achievable frequencies, the linear response of all block copolymers exhibits neither liquidlike terminal flow nor solidlike elasticity. The behavior falls somewhere between these limits depending upon the morphology and degree of long-range order. Topological defects such as dislocations, disclinations, and grain boundaries have been suggested to influence the low-frequency behavior,[1−3,6−8] but the nature of this connection remains obscure. Steady-shear studies of block copolymers have principally focused on the lamellar and cylindrical morphologies, sheared at relatively high rates;[1−3,9−13] published studies of bcc mesophase melts under large-amplitude reciprocating shear[7,8] also employed high rates. The present article examines the behavior of the bcc mesophase under steady shear, revealing a Newtonian region at the lowest stresses, followed by a "shear melting" of the bcc lattice as stress is increased.

Table 1. Physical Characteristics of Block Copolymers Studied

polymer code	wt % styrene	total mol wt (kg/mol)		T_{ODT} (°C) measured by	
		$\bar{M}_n$	$\bar{M}_w$	rheometry	SAXS
S/I 7/46	13.0	51.5	52.9	110 ± 2	111 ± 2
S/I 9/57	13.5	64.3	65.9	156 ± 2	161 ± 2
S/I 60/7	89.0	64.9	67.7	165 ± 2	165 ± 2
S/I 10/69	13.1	76.7	79.0	197 ± 2	202 ± 2
S/I/S 9/120/9	13.0	133.3	137.8	164 ± 2	167 ± 2

II. Experimental Section

A. Materials. A series of bcc-forming S/I diblock and S/I/S triblock copolymers were anionically polymerized by DEXCO Polymers (Plaquemine, LA). Characterization data for several of these polymers have been reported previously.[14−16] Compositions were determined by ^{1}H NMR in $CDCl_3$; all the I blocks are high (93%) in 1,4 addition. True molecular weights (Table 1) and polydispersities (<1.03 for all polymers) were determined via gel permeation chromatography (GPC) in toluene, using narrow-distribution S and I standards.[17] Materials are identified as S/I m/n, where m and n are the approximate $\bar{M}_w$ values of the S and I blocks in kg/mol. SAXS shows that all these polymers form the bcc mesophase at equilibrium and at low temperatures;[15] the order−disorder transition temperatures T_{ODT} (Table 1) were determined by SAXS and confirmed by rheometry.[14,15] All materials contained a commercial stabilizer package; GPC showed that even after testing at 150

† Department of Chemical Engineering.
‡ Princeton Materials Institute.
§ Present address: 3M Corporate Research, Science Research Center, St. Paul, MN 55144.
⊥ Present address: Bristol-Myers Squibb Pharmaceutical Research Institute, P.O. Box 191, New Brunswick, NJ 08903.
Present address: Dow-DuPont Elastomers L. L. C., P.O. Box 400, Plaquemine, LA 70765.
* To whom correspondence should be addressed. E-mail register@princeton.edu, tel (609) 258-4691.

10.1021/ma011522h CCC: $22.00
Published on Web 02/21/2002

°C for 3−5 days, little to no degradation had occurred (<10%). All rheological testing was done at temperatures above the glass transition temperature of the S phase, which is significantly depressed in these block copolymers relative to polystyrene homopolymer.[18,19]

B. Rheological Measurements. Controlled-stress measurements were performed on a DSR-200 (Rheometric Scientific, Piscataway, NJ), in a cone-and-plate geometry (2.3° gap angle, 40 mm diameter, or 5.7° gap and 25 mm diameter) with a temperature resolution of ±0.5 °C. In steady mode, the shear viscosity was measured for $10 \le \tau \le 10^3$ Pa. In dynamic oscillatory mode, the storage ($G'(\omega)$) and loss ($G''(\omega)$) moduli were measured over $10^{-2} \le \omega \le 10^2$ rad/s. Dynamic stress sweeps at $\omega \approx 10^{-2}$ rad/s, conducted on each polymer at each test temperature, verified that the stress amplitude employed (producing a strain amplitude ≈ 0.5%) remained within the linear regime. Controlled-rate and stress relaxation measurements were performed with an RMS-800 (Rheometric Scientific), with a temperature resolution of ±1 °C. A parallel plate geometry (25 mm diameter) was used for dynamic oscillatory measurements and a cone-and-plate geometry (5.7° gap and 25 mm diameter) for steady-shear measurements.

Specimens were compression-molded under vacuum into disks and loaded into the rheometer. To ensure that the equilibrium mesophase morphology was attained, samples were heated in the rheometer to at least 5 °C above T_{ODT} for 15 min and then quenched to the desired testing temperature, and the dynamic moduli were monitored at $\omega \approx 10^{-2}$ rad/s until both moduli attained their limiting values.[6,15] When changing test temperature, careful attention was paid to maintaining a constant gap spacing to ensure that the sample's shape was not distorted significantly. All experiments were conducted under a continuous nitrogen purge.

C. Small-Angle X-ray Scattering. Ex-situ SAXS measurements were conducted following testing in the DSR. Only the triblock S/I/S 9/120/9 could be removed intact from the rheometer, as the diblocks have little mechanical strength. Specimens of S/I/S 9/120/9 were quenched in the DSR from the testing temperature to room temperature at 10 °C/min. SAXS measurements were made at room temperature, using a compact Kratky camera and a one-dimensional position-sensitive detector (Braun OED-50M).[20] Data were corrected for empty beam scattering, detector sensitivity, and positional linearity, desmeared for slit length, and placed on an absolute intensity scale.[20] Intensities are presented vs scattering vector $q = (4\pi/\lambda) \sin\theta$, where λ is the radiation wavelength (Cu Kα) and 2θ is the scattering angle.

III. Results and Discussion

A. Linear Viscoelastic Behavior. Block copolymers having a bcc lattice morphology are known to manifest a low-frequency (long time) plateau modulus G^0_{bcc} whose magnitude is directly related to the size of the lattice unit cell.[1−3,6] Such behavior is commonly encountered in other "soft" systems containing a three-dimensional lattice, such as colloidal and micellar cubic crystals.[1,2,21,22] At very low frequency, however, the plateau modulus begins to fall below G^0_{bcc}. Figure 1 shows a dynamic frequency sweep on S/I 9/57, where the complex modulus $G^*(\omega) = \sqrt{G'(\omega)^2 + G''(\omega)^2}$ falls away from G^0_{bcc} at $\omega < 10^{-2}$ rad/s. Similarly, in stress relaxation experiments, the relaxation modulus $G(t)$ falls below G^0_{bcc} at long times (Figure 1).

A recent study[6] has suggested that defects permit long-time relaxations in cubic-phase block copolymers, leading to a crossover from solidlike to liquidlike terminal behavior at sufficiently low frequency. However, true terminal behavior in bcc melts has not yet been demonstrated; it appears to lie below the range of frequencies measurable with standard instrumentation.[1,3,6,23] The DSR does not function below 10^{-4} rad/s, and already at 10^{-3} rad/s the reproducibility is poor. In addition, strain amplitudes large enough to accurately record can exceed the linear viscoelastic limit, which becomes lower at lower frequency.[6] Transient measurements, such as stress relaxation, are plagued by complementary problems: if the initial stress is kept small enough that it lies within the linear regime, then at the long times where terminal behavior is approached (>10^4 s) the torque falls below the detection limits of the RMS-800's transducer. Thus, at best, oscillatory and relaxation measurements can only suggest the existence of terminal-type behavior in ordered block copolymer melts, so they were not employed in the present study. As an aside, however, we have found that bcc-forming concentrated solutions of a block copolymer in a selective solvent can exhibit accessible liquidlike terminal linear viscoelastic behavior.[24]

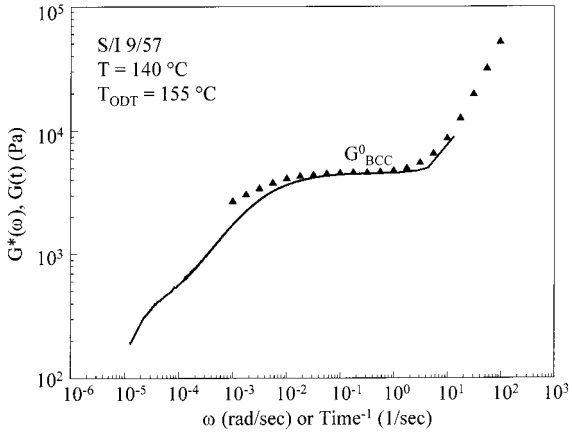

Figure 1. Complex storage modulus $G^*(\omega)$ (▲) and relaxation modulus $G(t)$ (—) for diblock S/I 9/57 in its fully ordered state at 140 °C. $G(t)$ has been plotted against 1/time to facilitate comparison with $G^*(\omega)$.

B. Steady-Shear Rheology. We chose to employ steady-shear measurements in part because significantly lower deformation rates are obtainable than in dynamic oscillatory measurements (10^{-7} s^{-1} vs 10^{-4} rad/s). More importantly, however, steady-shear testing with a controlled-stress instrument is the most sensitive method to probe the low-deformation-rate behavior of a material, because it allows for the precise measurement of a yield stress, if present—a measurement impossible with a controlled-strain instrument.[11,25−27]

Creep tests were made starting from low τ (≈10 Pa) and increasing to the DSR's limit (1000 or 4000 Pa, depending on cone diameter). At each τ the shear strain $\gamma(t)$ was measured until a steady shear rate $\dot\gamma$ was attained, yielding the steady-state viscosity η. Representative creep and recovery curves for S/I 10/69 are shown in Figure 2. Measurements at the lowest τ often did not exhibit the completely smooth creep curves typical for simple viscous flow even after prolonged periods of shearing. These $\dot\gamma$ fluctuations do not appear to be an instrument artifact, as creep tests performed on a polystyrene homopolymer of equivalent η and at equally low $\dot\gamma$ were smooth. As τ was increased, smoother $\gamma(t)$ curves were obtained.[28]

Figure 3 shows η vs τ for S/I 10/69 at five temperatures. This uncommon manner of presenting the flow curve was chosen because it more clearly illustrates the dramatic changes which occur in the rheology. Proceeding from low to high τ, three distinct regimes can be seen. At low τ, η exhibits a Newtonian viscosity plateau

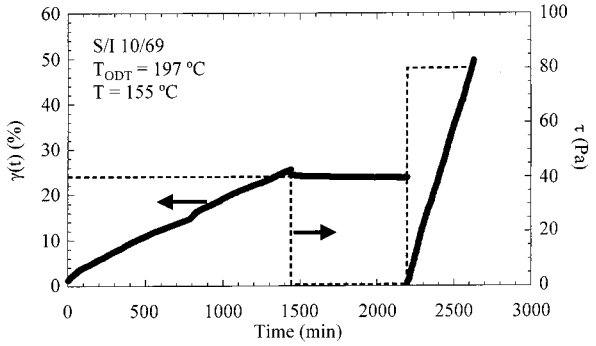

Figure 2. Creep behavior of S/I 10/69 at 155 °C. Applied shear stress τ shown as dashed lines; strain $\gamma(t)$ shown by symbols forming thick lines. Note steady creep at τ of both 40 and 80 Pa.

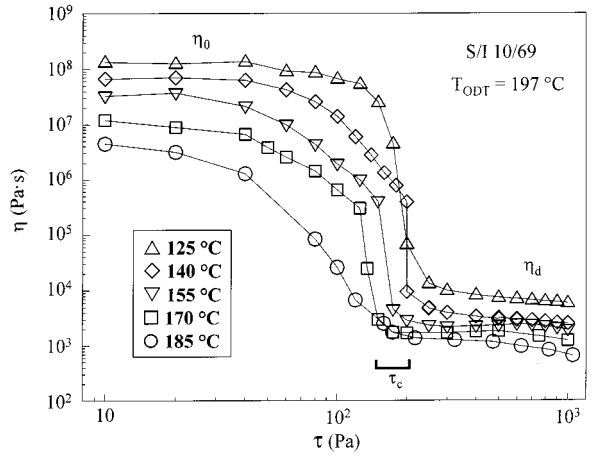

Figure 3. Flow curves $\eta(\tau)$ of ordered diblock S/I 10/69 at various temperatures below its T_{ODT}. η_0 represents the low-stress regime, η_d represents the high-stress regime, and the critical shear stress τ_c designates the transition regime.

on the order of 10^7-10^8 Pa·s. In the ensuing discussion, this region is referred to as the low-stress regime, characterized by a zero-shear viscosity η_0. As τ is increased, there is a dramatic drop in η over a narrow range of τ at approximately 200 Pa; in this range, a factor of 3 increase in τ causes a decrease in η by roughly 4 orders of magnitude. This portion of the flow curve is termed the transition regime and is characterized by a critical stress (τ_c). As τ is increased further, a weakly shear-thinning region is entered, termed the high-stress regime. In this regime, η is in the range of 10^3-10^4 Pa·s, and the behavior is similar to that of a simple homopolymer.

The steady-shear behavior of a bcc-forming triblock copolymer melt was also investigated. Figure 4 compares the flow curves of a matched diblock−triblock pair (S/I 9/57 and S/I/S 9/120/9), where the triblock chain is nearly equivalent to two diblock chains coupled together at their I ends (i.e., $\bar{M}_{w,triblock} \approx 2\bar{M}_{w,diblock}$). Qualitatively, both systems show the same behavior as was found for S/I 10/69, indicating that the same flow mechanisms are present for both diblock and triblock copolymer melts in the ordered state. This may appear surprising, since it indicates that chains which bridge S domains in the triblock system (and are responsible for the good elastomeric properties at room temperature) do not produce any qualitative differences in the steady-shear melt rheology. This similarity in rheology between diblock and triblock architectures indicates that diffusion of individual chains through the lattice occurs more rapidly than the time scales probed here, such that end blocks do not remain associated with a particular microdomain long enough to impact the low-shear-rate response. Consistent with this conclusion, diblocks and triblocks of similar sphere-forming block length have recently been shown to diffuse through a spherical microdomain structure at similar rates.[32]

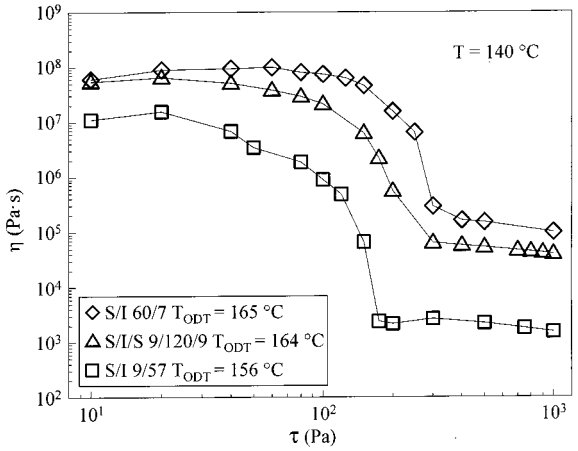

Figure 4. Flow curves $\eta(\tau)$ at 140 °C for ordered diblocks S/I 9/57 (□) and S/I 60/7 (◇) and triblock S/I/S 9/120/9 (△).

To further investigate how architecture affects the flow behavior of bcc-forming block copolymer melts, a diblock copolymer (S/I 60/7) which forms I spheres in an S matrix—the compositional "inverse" of the materials discussed thus far, but with a similar molecular weight to S/I 9/57—was examined. Figure 4 shows that the S-rich and I-rich diblocks exhibit similar flow curves, with the primary difference being a higher viscosity for the S-rich diblock. Even this difference is reasonable, given the closer proximity to the polystyrene glass transition temperature.

Having established the existence of these three regimes of flow behavior in a range of bcc-forming melts, we sought a microscopic structural explanation through SAXS measurements on the triblock S/I/S 9/120/9. The sluggish ordering kinetics[15] of this polymer permit it to be quenched in the rheometer and removed for ex-situ SAXS without significant structural change. Figure 5 displays the SAXS patterns for S/I/S 9/120/9 measured after shear histories corresponding to each of the three flow regimes at 120 °C. Profiles have been shifted along the intensity axis for clarity. Profile a was taken after shearing the system in the low-stress regime, profile b after shearing in the transition regime, and profile c after shearing in the high-stress regime. Profiles a and b show a narrow primary peak at q^* and higher-order peaks at q/q^* ratios of $1:\sqrt{2}:\sqrt{3}$, indicating that the material still possesses bcc lattice order during flow. After shearing in the high-stress region, however, the main peak is broadened and shifted to slightly higher q, and the higher-order peaks disappear. For comparison, profile d was obtained for a specimen which was thermally disordered by heating above T_{ODT} and quenching to room temperature. Profiles c and d can be quantitatively modeled as the scattering from an assembly of spheres possessing liquidlike order[15,33] and are typical of the SAXS patterns obtained for highly asymmetric block copolymers disordered by heating to slightly above their ODT temperatures.

Figure 5 shows that shearing at $\tau > \tau_c$ destroys the bcc lattice, producing a structure analogous to that

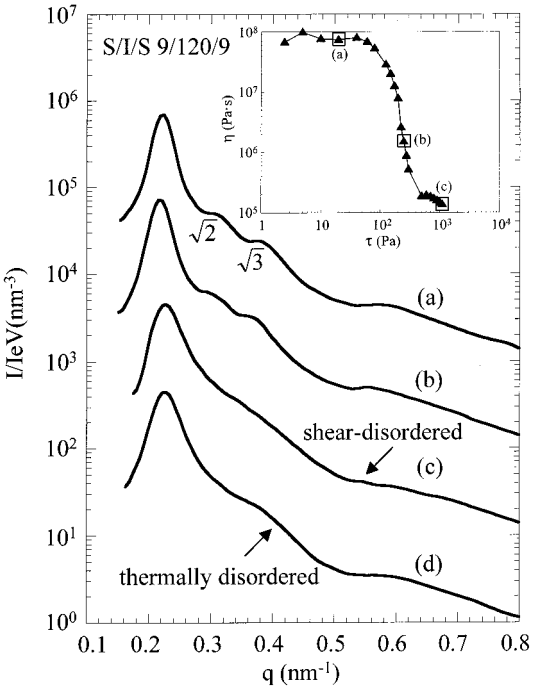

Figure 5. Room temperature SAXS patterns for triblock S/I/S 9/120/9 taken after various shear and thermal histories. Inset shows the flow curve at 120 °C and the corresponding locations of the three shear stresses employed. Profile a was taken after shearing at 20 Pa for 12 h (120 °C). Profile b was taken after shearing at 100 Pa for 1 h (120 °C). Profile c was taken after shearing at 1000 Pa for 30 min (120 °C). Profile d was taken after holding the system at 120 °C for 200 min following a quench from 180 °C ($> T_{ODT}$). For clarity, each profile after (a) has been successively shifted downward by a factor of 10 in intensity.

obtained by thermal disordering. Such a "shear melting" has been observed previously in steady shear for certain colloidal systems,[25,34−36] but not for diblock copolymer melts. In fact, shearing of lamellar or cylindrical diblock melts produces a modest stabilization of the ordered structure.[37−41] By contrast, lamellar triblocks subjected to reciprocating shear do show a destabilization of the ordered phase, once the rate of entanglement relaxation becomes comparable to the characteristic deformation rate.[42] The qualititative difference between lamellar diblocks vs triblocks (stabilization vs destabilization) underscores the difference between the disordering process for lamellar structures and the one we observe for sphere-forming block copolymers, where diblocks and triblocks behave similarly (see Figure 4). The most pertinent prior report is that of Koppi et al.,[9] who observed a disordering in aligned bcc-phase diblock copolymers when subjected to large-amplitude reciprocating shear at an intermediate shear rate. However, because cessation of shear led to the redevelopment of the original ordered structure, the authors concluded that their observations arose from slippage of planes of spheres past each other in the shear direction, rather than a complete disordering. Since reciprocating shear is limited in its amplitude, it is possible that the material does not achieve steady state prior to the reversal of flow; indeed, at higher shear rates, Koppi et al. observed no disordering because the specimen simply deformed elastically up to the full strain amplitude. The time dependence of the shear disordering we observe (on unoriented specimens) is discussed briefly below and more fully in a companion paper.[43]

With this structural basis for the observed rheological transitions in mind, we return to each of the three flow regimes to examine the rheological behavior in greater detail and to demonstrate that this shear-disordering phenomenon is equivalent to the well-studied thermal disordering of these block copolymers.

(a) Low-Stress Regime. The presence of an η_0 plateau in ordered bcc-forming block copolymer melts demonstrates that these materials, despite the presence of a lattice structure, do not exhibit simple yield stress behavior (i.e., no flow for sufficiently small τ). The Newtonian behavior seen in Figures 3 and 4 is also consistent with an extrapolation of Figure 1, which suggests that terminal behavior would be achieved if measurements could be made at much lower frequencies.

Since SAXS indicates that the lattice structure is retained during flow, one expects a portion of the macroscopic deformation to be associated with deformation of the lattice. This portion of the deformation should be essentially elastic (instantaneous recovery),[27] with a modulus equal to G^0_{bcc}. Recovery measurements were performed following creep tests at low τ, as shown in Figure 2 for S/I 10/69. After shearing the diblock at $\tau =$ 40 Pa for 24 h (corresponding to a strain of 0.255 and an average viscosity 1.5×10^7 Pa·s), the stress was released and the polymer allowed to recover. The recoverable elastic strain γ_r was found to be 0.018, in reasonable agreement with the initial elastic strain $\gamma_e = \tau/G^0_{bcc} = 0.015$. This agreement confirms that the ex-situ SAXS measurements reflect the actual structure during shear: that is, the bcc lattice is not destroyed, provided $\tau < \tau_c$.

The large magnitude of η_0 in the low-stress regime, coupled with the presence of an ordered lattice, suggests a defect-mediated flow mechanism such as grain boundary sliding, vacancy motion, or dislocation movement, which are also known to occur in other ordered materials such as colloidal suspensions, micellar crystals, metals, and ceramics.[34,35,44−46] We defer further examination of this subject to a future paper.[24]

(b) Transition Regime. The values of η which we report in this regime are the steady-state values; they are maintained during shearing at the given τ for extended periods and are reproducible between runs. However, achieving a steady state in the transition regime following a step increase in stress required shearing for unusually long periods (up to 8 h), during which time the apparent viscosity steadily decreased. We assign the value of the critical stress τ_c as that where η declines most steeply; τ_c occurs near the end of the transition regime. As shown in Figure 3, τ_c depends weakly on temperature. Because τ_c is related to the strength of the bcc lattice, it is reasonable that its magnitude should be related to G^0_{bcc}, a property which also shows a weak dependence on temperature.[3] In the companion paper,[43] we discuss the relationship between G^0_{bcc} and τ_c, drawing analogies with other crystalline materials such as metals, ceramics, and colloids.

To determine how this flow transition progresses as a function of shear rate rather than shear stress, controlled-rate measurements were made on the RMS-800. For S/I 10/69 at 155 °C, the lowest shear rate which gave a detectable torque signal was 5×10^{-5} s^{-1}. Shear rates were incrementally increased from this level up to $\approx$1 s^{-1}, generating the flow curve shown in Figure 6, overlaid on the flow curve obtained from the corre-

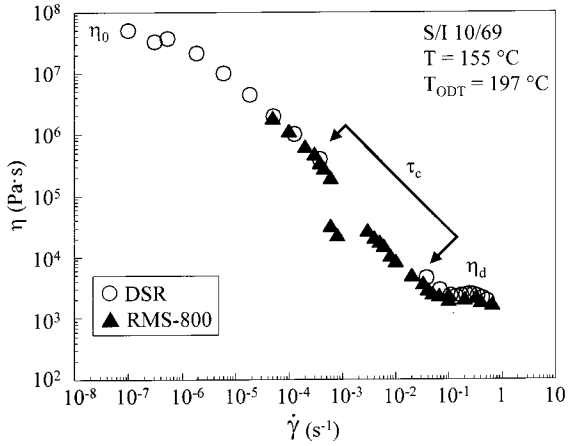

Figure 6. Comparison of flow curves $\eta(\dot{\gamma})$ for S/I 10/69 at 155 °C measured using the controlled-stress DSR (○) and the controlled-strain-rate RMS-800 (▲).

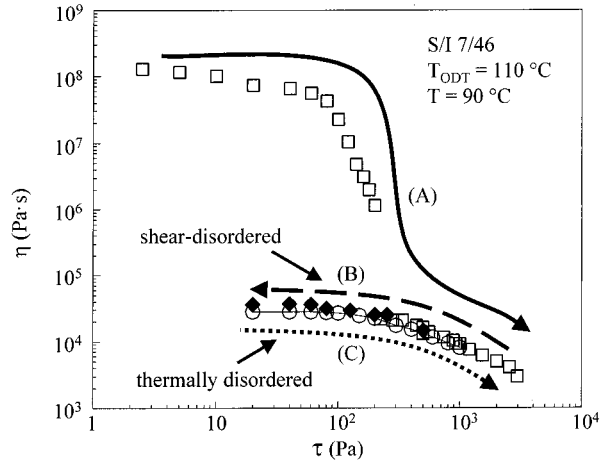

Figure 7. Flow curves $\eta(\tau)$ for diblock S/I 7/46 measured at 90 °C after various shear and thermal histories. For path A, η was measured from low to high τ (□); for path B, η was measured from high to low τ (◆) to probe the shear-disordered state. For path C, η was measured from low to high τ (○) for a specimen quenched into the thermally disordered metastable state via a quench from 110 °C ($> T_{ODT}$).

sponding test done on the controlled-stress DSR. The flow curve obtained on the DSR contains a gap in the measured shear rates, $4 \times 10^{-4}\ s^{-1} < \dot{\gamma} < 4 \times 10^{-2}\ s^{-1}$, which corresponds to the steep viscosity drop at τ_c. In contrast, the flow curve generated via the RMS-800 is continuous across the entire range of shear rates, but the response is erratic in the region right around τ_c, due to the usual transient stress overshoot when the shear rate is increased. Similar behavior has been reported for colloidal suspensions where a transition from polycrystalline flow to a layer-sliding mechanism occurs at a dynamic yield stress.[47−51]

(c) High-Stress Regime. At stresses above τ_c, the block copolymers all enter a weakly shear-thinning region which persists up to the testing limits of the DSR (Figures 3 and 4). The slow ordering rate of these materials[15] suggests that if one were to reduce the stress back below τ_c, the viscosity should show pronounced hysteresis, a property common in colloidal systems.[34] Figure 7 shows this effect for S/I 7/46 at 90 °C, where in path A, τ was continuously increased from zero, while in path B, τ was continuously decreased from 3000 Pa ($\tau > \tau_c$). At high τ, the two paths coincide, indicating that shear history does not affect this portion of the flow curve. At $\tau < \tau_c$, however, η_0 is roughly 3 orders of magnitude lower when starting from a shear-disordered state ($\tau > \tau_c$) than when starting from a quiescently ordered state ($\tau = 0$). Along path B, the flow curve is quite similar to that of a simple shear-thinning polymeric system with no viscosity transition region.

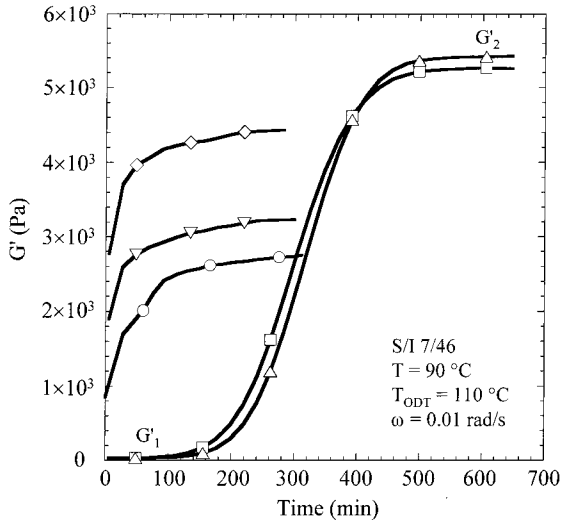

Figure 8. Temporal evolution of dynamic storage modulus G' at 0.01 rad/s for the diblock S/I 7/46 at 90 °C after various shear and thermal histories: (△) after a quench from the thermally disordered state at 115 °C, (□) after shearing at 500 Pa for 20 min, (◇) after shearing at 250 Pa for 30 min, (▽) after shearing at 250 Pa for 2 h, and (○) after large-amplitude oscillatory shear at $\gamma_0 = 100\%$ and $\omega = 2$ rad/s for 45 min. G'_1 represents the disordered metastable state, and G'_2 represents the equilibrium, unaligned bcc-ordered state at 90 °C. For clarity, only a few symbols are indicated on each ordering curve; the actual density of points is one per 20 min.

To explore the similarities between the shear-disordered and thermally disordered states, S/I 7/46 was thermally disordered by heating to 110 °C and then quenched to 90 °C, the same temperature at which the flow curves in Figure 7 were measured. Viscosity measurements were then made from low to high stress while the polymer was still in its thermally disordered metastable state; the slow ordering kinetics of this polymer at 90 °C (ordering half-time[15] ≈ 300 min) permit such measurements, as the stress sweeps shown in Figure 7 for both disordered specimens required only 100−120 min to conduct over the range $\tau < \tau_c$. The flow curve of this thermally disordered metastable specimen (path C in Figure 7) is indistinguishable from the flow curve of the shear-disordered material (path B). Consistent with the SAXS results of Figure 5, the flow curves of Figure 7 indicate that the shear-disordered and thermally disordered states are indistinguishable.

(d) Ordering Kinetics. If a bcc-forming block copolymer is quenched from $T > T_{ODT}$ to $T < T_{ODT}$, the equilibrium ordered structure does not develop immediately, due to the sluggish diffusion of polymer chains.[15] The ordering kinetics can be tracked through time-resolved measurements of G' at a fixed (low) frequency. Figure 8 shows a typical isochronal dynamic time sweep, for S/I 7/46 at 90 °C following a quench from 110 °C. At short times, G' exhibits a low-magnitude plateau (G'_1) characteristic of the metastable disordered state. At long times, a higher-magnitude G' plateau is reached (G'_2), which signifies that the bcc lattice has fully formed. We define the ordering half-time ($t_{1/2}$) as the time when G' reaches the average of its short- and

long-time plateaus, $G'_{1/2} = (G'_1 + G'_2)/2$. If the shear-disordered and thermally disordered states are equivalent, then one would expect the reordering rates from these two states to be identical. Figure 8 also shows data for S/I 7/46 at 90 °C, sheared steadily for 20 min at $\tau =$ 500 Pa ($>\tau_c$) and then monitored by time-resolved dynamic oscillatory measurements in the linear regime. This curve closely tracks that following the thermal quench from the disordered state, and the two show identical half-times to within experimental error (328 min after shear-disordering vs 348 min after thermally disordering).

Shearing the system into the transition regime generates a partially disordered state, similar to the continuous disordering progression occurring in some colloidal systems.[36,51] The SAXS data in Figure 5 reflect this, as the higher-order peaks in profile b are weaker than in profile b; indeed, profile b can be adequately described by a linear combination of the scattering from ordered (profile a) and shear-disordered (profile c) specimens. This partial disordering is also evident rheologically. In Figure 8, two additional curves show the ordering behavior of S/I 7/46 after being sheared at 250 Pa for 30 min and for 2 h. Though this stress slightly exceeds τ_c, approximately 7 h is required for η to achieve its steady-state value at this applied stress, and thus shearing for 30 min or 2 h does not fully disorder the material. This is reflected rheologically in the short-time value of G', which greatly exceeds G'_1 and rises very quickly with time. However, the limiting values of G' attained at long times are significantly less than the long time G'_2 plateau (G^0_{bcc}) measured after reordering from a fully disordered state. This suggests that the partially disordered systems reorder with an aligned microstructure, rather than the random arrangement of grains whose ensemble yields G^0_{bcc}.

We hypothesize that the regions of the specimen which remain ordered during shearing in the transition regime act as nuclei during the reordering process, producing the accelerated ordering rates seen in Figure 8 relative to the case where the material started from the fully disordered state. Furthermore, these nuclei could easily be aligned during the shear, yielding an aligned microstructure after reordering. To quantify the effect of flow alignment on rheological response for S/I 7/46, an additional specimen was first aligned using large-amplitude oscillatory shear[7,8] (LAOS; $\gamma_0 = 100\%$, 2 rad/s) and then its response monitored with small-amplitude oscillatory shear. As shown in Figure 8, LAOS can produce an equilibrium modulus which is approximately 50% less than G^0_{bcc}. Interestingly, the structure immediately following LAOS also appears to be partially disordered, as G' rises with a time course similar to the specimens which were partially disordered by steady shear.

All the data in Figure 8 were generated by monitoring the system with small-amplitude oscillatory shear, essentially a zero-stress condition. However, one might suspect that shear-disordered systems would be able to reorder even if kept under steady shear, provided the stress is reduced to $\tau < \tau_c$. The inset of Figure 9 shows the temporal evolution of the viscosity for S/I 7/46 at 90 °C under continuous steady shear. The material was first shear-disordered by applying 500 Pa ($>\tau_c$) for 20 min, after which it was sheared at 40 Pa ($\tau < \tau_c$). At short times, η is low ($\equiv\eta_1$), signifying that the system is in its shear-disordered state; indeed, this value of η_1 equals the zero-shear viscosity found on path B in Figure 7. At longer times, η rises until it reaches a second plateau value ($\equiv\eta_2$), indicating that the bcc order in the system has returned. This type of test was repeated at several other $\tau < \tau_c$, and similar sigmoidal reordering curves were observed, though with slightly different rates which are conveniently quantified with a viscosity half-time analogous to the modulus half-time extracted from the data of Figure 8. Figure 9 shows the $t_{1/2}$ values determined under steady shear at various τ following shear disordering; the dependence of $t_{1/2}$ on τ is essentially linear for the values of τ employed and extrapolates to $t_{1/2} = 321$ min at $\tau = 0$. This value may be compared directly with other zero-stress measurements of the reordering time (also plotted in Figure 9): $t_{1/2} = 328$ min for a sample shear disordered and monitored by small-amplitude oscillatory shear, $t_{1/2} =$ 348 min for a sample thermally disordered and monitored by small-amplitude oscillatory shear, and $t_{1/2} =$ 270 min previously reported[15] for a sample thermally disordered and monitored by SAXS. The excellent agreement between all these values emphasizes the equivalence of the shear-disordered and thermally disordered metastable states. While the limit of this linear dependence of $t_{1/2}$ on τ has not been determined, we presume that, at stresses approaching τ_c, $t_{1/2}$ will diverge.

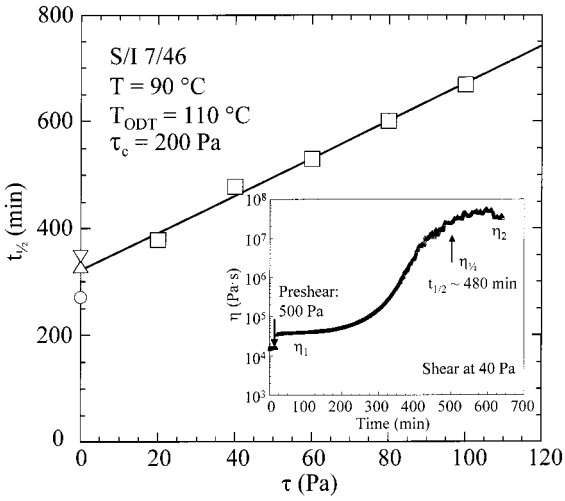

Figure 9. Ordering half-times $t_{1/2}$ for diblock S/I 7/46 at 90 °C as a function of shear stress τ applied during the ordering process (□). As shown in the inset, measurements were taken after shearing at 500 Pa ($>\tau_c$) for 20 min to induce shear disordering. The stress was then reduced below τ_c, and the temporal evolution of η was monitored, where η_1 represents the shear-disordered metastable state and η_2 represents the steady-state η after reordering. Values of $t_{1/2}$ obtained from dynamic oscillatory measurements (Figure 8) after shear disordering (△) and after thermal disordering (▽) and from SAXS measurements taken after thermal disordering[15] (○) are shown for comparison at $\tau = 0$.

IV. Conclusions

The steady-shear rheology of bcc-forming block copolymer melts is directly dependent on the state of mesophase order present in the system, and its progression with increasing deformation rate divides into three distinct regions. At low stresses, the bcc lattice remains intact, and flow occurs by a creeping relaxation mechanism with an essentially Newtonian viscosity. This relaxation mechanism is responsible for the previously reported decay in the modulus below G^0_{bcc} at low fre-

quencies, the absence of a true yield stress as demonstrated here, and the very large magnitude of the viscosity measured in this regime (10^7-10^8 Pa·s). As the stress is increased, the bcc lattice is disrupted, causing the viscosity to decrease. This shear-disordering process occurs over a very narrow span of stress and is characterized by a critical stress beyond which the system no longer possesses any mesophase order. At still higher stresses, the system behaves as a simple shear-thinning polymeric material. This shear-disordered state is metastable, equivalent both rheologically and structurally to the thermally disordered metastable state. If the shear-disordered system is held below the critical stress, it orders back to the bcc structure with kinetics analogous to those exhibited after thermal disordering. Furthermore, over a substantial range of stress, the ordering time appears to be linear in the applied stress.

Acknowledgment. This work was supported by the National Science Foundation through the Princeton Center for Complex Materials (DMR-9400362 and -9809483) and a Graduate Fellowship (to J.M.S.). The authors thank Professor William B. Russel for helpful discussions.

References and Notes

(1) Hamley, I. W. *The Physics of Block Copolymers*; Oxford University Press: Oxford, 1998.
(2) Colby, R. H. *Curr. Opin. Colloid Interface Sci.* **1996**, *1*, 454.
(3) Fredrickson, G. H.; Bates, F. S. *Annu. Rev. Mater. Sci.* **1996**, *26*, 501.
(4) Holden, G., Legge, N. R., Quirk, R., Schroeder, H., Eds.; *Thermoplastic Elastomers*, 2nd ed.; Hanser/Gardner Publications: Cincinnati, OH, 1996.
(5) Larson, R. G. *Structure and Rheology of Complex Fluids*; Oxford University Press: New York, 1999.
(6) Kossuth, M. B.; Morse, D. C.; Bates, F. S. *J. Rheol.* **1999**, *43*, 167.
(7) Almdal, K.; Koppi, K. A.; Bates, F. S. *Macromolecules* **1993**, *26*, 4058.
(8) Koppi, K. A.; Tirrell, M.; Bates, F. S.; Almdal, K.; Mortensen, K. *J. Rheol.* **1994**, *38*, 999.
(9) Kraus, G.; Naylor, F. E.; Rollman, K. W. *J. Polym. Sci., Part A-2* **1971**, *9*, 1839.
(10) Han, J. H.; Feng, D.; Choi-Feng, C.; Han, C. D. *Polymer* **1995**, *36*, 155.
(11) Hansen, P. J.; Williams, M. C. *Polym. Eng. Sci.* **1987**, *27*, 586.
(12) Chung, C. I.; Gale, J. C. *J. Polym. Sci., Polym. Phys. Ed.* **1976**, *14*, 1149.
(13) Holden, G. In *Block and Graft Copolymerization*; Ceresa, R. J., Ed.; John Wiley & Sons: London, 1974; Vol. 1, p 133.
(14) Adams, J. L.; Graessley, W. W.; Register, R. A. *Macromolecules* **1994**, *27*, 6026.
(15) Adams, J. L.; Quiram, D. J.; Graessley, W. W.; Register, R. A.; Marchand, G. R. *Macromolecules* **1996**, *29*, 2929.
(16) The polyisoprene GPC calibration standards used previously in determining the molecular weights of some of these polymers suffered from a systematic error in molecular weight. We have recently redetermined[17] the molecular weights of the polymers having approximately 13 wt % S block and found the original values[14,15] to be ca. 18% high (for example, S/I 10/69, previously coded as D90, was previously reported to have $M_n = 90.6$ kg/mol, vs our current best estimate of 76.7 kg/mol).
(17) Sebastian, J. M.; Register, R. A. *J. Appl. Polym. Sci.* **2001**, *82*, 2056.
(18) Spaans, R. D.; Williams, M. C. *Ind. Eng. Chem. Res.* **1995**, *34*, 3496.
(19) Granger, A. T.; Wang, B.; Kraus, S.; Fetters, L. J. In *Multicomponent Polymer Materials*; ACS Symposium Series 211; Paul, D. R., Sperling, L. H., Eds.; American Chemical Society: Washington, DC, 1986; p 127.
(20) Register, R. A.; Bell, T. R. *J. Polym. Sci., Polym. Phys.* **1992**, *30*, 569.
(21) Russel, W. B.; Saville, D. A.; Schowalter, W. R. *Colloidal Dispersions*; Cambridge University Press: Cambridge, 1989.
(22) Buitenhuis, J.; Förster, S. *J. Chem. Phys.* **1997**, *107*, 262.
(23) Zhao, J.; Majumdar, B.; Schulz, M. F.; Bates, F. S.; Almdal, K.; Mortensen, K.; Hajduk, D. A.; Gruner, S. M. *Macromolecules* **1996**, *29*, 1204.
(24) Sebastian, J. M.; Graessley, W. W.; Register, R. A., submitted to *J. Rheol.*
(25) Watanabe, H.; Kotaka, T. *Polym. Eng. Rev.* **1984**, *4*, 73.
(26) Nguyen, Q. D.; Boger, D. V. *Annu. Rev. Fluid Mech.* **1992**, *24*, 47.
(27) Eiser, E.; Molino, F.; Porte, G.; Pithon, X. *Rheol. Acta* **2000**, *39*, 201.
(28) At such low deformation rates and high apparent viscosities, one might be concerned that the observed motion actually reflects slip of a true yield-stress fluid at the tool surfaces or some other measurement artifact. To test this idea,[29] "creep" tests were conducted on a commercial polystyrene homopolymer at temperatures close to its T_g (≈100 °C). All showed a wholly elastic response with no discernible creep, indicating that a true solidlike response will be measured as such. Second, creep tests were also performed on this polystyrene at 135 °C, chosen via correlations reported in the literature[30] to yield $\eta_0 = 1.2 \times 10^8$ Pa·s for the known $\bar{M}_w$. Not only did our viscosity measurements ($\eta_0 = 1.1 \times 10^8$ Pa·s) agree well with the predicted value, but they also agreed with corresponding dynamic oscillatory measurements as expected by the Cox−Merz rule.[31] While neither of these tests explicitly rules out slip at the tool faces, we note that the reproducibility in the data (especially when using cones of two different diameters) and the smooth temperature dependence of the measurements shown in Figure 3 are not characteristic of this artifact.
(29) Sebastian, J. M. Ph.D. Thesis, Princeton University, 2001.
(30) Fox, T. G.; Gratch, S.; Loshaek, S. In *Rheology Theory and Applications*; Eirich, F. R., Ed.; Academic Press: New York, 1956; Vol. 1, p 431.
(31) Cox, W. P.; Merz, E. H. *J. Polym. Sci.* **1958**, *28*, 619.
(32) Yokoyama, H.; Kramer, E. J. *Macromolecules* **2000**, *33*, 954.
(33) Kinning, D. J.; Thomas, E. L. *Macromolecules* **1984**, *17*, 1712.
(34) McConnell, G. A.; Lin, M. Y.; Gast, A. P. *Macromolecules* **1995**, *28*, 6754.
(35) Chen, L. B.; Chow, M. K.; Ackerson, B. J.; Zukoski, C. F. *Langmuir* **1994**, *10*, 2817.
(36) van der Vorst, B.; van den Ende, D.; Aelmans, N. J. J.; Mellema, J. *Phys. Rev. E* **1997**, *56*, 3119.
(37) Koppi, K. A.; Tirrell, M.; Bates, F. S. *Phys. Rev. Lett.* **1993**, *70*, 1449.
(38) Nakatani, A.; Morrison, F.; Douglas, J.; Mays, J.; Jackson, C.; Muthukumar, M.; Han, C. C. *J. Chem. Phys.* **1996**, *104*, 1589.
(39) Jackson, C. L.; Morrison, F. A.; Nakatani, A. I.; Mays, J. W.; Muthukumar, M.; Barnes, K. A.; Han, C. C. In *Flow-Induced Structure in Polymers*; ACS Symposium Series 597; Nakatani, A. I., Dadmun, M. D., Eds.; American Chemical Society: Washington, DC, 1995; p 233.
(40) Balsara, N. P.; Hammouda, B.; Kesani, P. K.; Jonnalagadda, S. V.; Straty, G. C. *Macromolecules* **1994**, *27*, 2566.
(41) Bates, F. S.; Koppi, K. A.; Tirrell, M.; Almdal, K.; Mortensen, K. *Macromolecules* **1994**, *27*, 5934.
(42) Tepe, T.; Hajduk, D. A.; Hillmyer, M. A.; Weimann, P. A.; Tirrell, M.; Bates, F. S.; Almdal, K.; Mortensen, K. *J. Rheol.* **1997**, *41*, 1147.
(43) Sebastian, J. M.; Lai, C.; Graessley, W. W.; Register, R. A. *Macromolecules* **2002**, *35*, 2707.
(44) Langdon, T. G. *Mater. Trans., JIM* **1996**, *37*, 359.
(45) Cannon, W. R.; Langdon, T. G. *J. Mater. Sci.* **1988**, *23*, 1.
(46) Stevens, M. J.; Robbins, M. O.; Belak, J. F. *Phys. Rev. Lett.* **1991**, *66*, 3004.
(47) Chen, L. B.; Ackerson, B. J.; Zukoski, C. F. *J. Rheol.* **1994**, *38*, 193.
(48) Chen, L. B.; Zukoski, C. F.; Ackerson, B. J.; Hanley, H. J. M.; Straty, G. C.; Barker, J.; Glinka, C. J. *Phys. Rev. Lett.* **1992**, *69*, 688.
(49) Chen, L. B.; Zukoski, C. F. *J. Chem. Soc., Faraday Trans.* **1990**, *86*, 2629.
(50) Chen, L. B.; Zukoski, C. F. *Phys. Rev. Lett.* **1990**, *65*, 44.
(51) Imhof, A.; Vanblaaderen, A.; Dhont, J. K. G. *Langmuir* **1994**, *10*, 3477.

MA011522H